

# A Generic Two-band Model for Unconventional Superconductivity in Electron and Hole Doped Iron-Based Superconductors

Qiang Han,<sup>1</sup> Yan Chen,<sup>2</sup> and Z. D. Wang<sup>3,\*</sup>

<sup>1</sup>*Department of Physics, Renmin University, Beijing, China*

<sup>2</sup>*Department of Physics and Lab of Advanced Materials, Fudan University, Shanghai, China*

<sup>3</sup>*Department of Physics and Center of Theoretical and Computational Physics,  
The University of Hong Kong, Pokfulam Road, Hong Kong, China*

(Dated: April 14, 2019)

Based on experimental data on the newly synthesized iron-based superconductors and the relevant band structure calculations, we propose a minimal two-band BCS-type Hamiltonian with the interband Hubbard interaction included. We show that this two-band model is able to capture the essential features of unconventional superconductivity and spin density wave (SDW) ordering in this family of materials. It is found that bound electron-hole pairs can be condensed to reveal the SDW ordering for zero and very small doping, while the superconducting ordering with the  $d$ -wave pairing symmetry emerges at small finite doping. The derived analytical formulas not only give out a nearly symmetric phase diagram for electron and hole doping, but also is likely able to account for existing main experimental results. Moreover, we also derive two important relations for a general two-band model and elaborate how to apply them to determine the band width ratio and the effective interband coupling strength from experimental data.

PACS numbers: 74.20.Rp, 74.25.Bt, 65.40.Ba, 74.70.Dd

Since the recent discovery of a new iron-based layered superconductor<sup>1</sup>, intensive efforts have been focused on the nature of superconductivity in this materials both experimentally<sup>2,3,4,5,6,7,8,9,10,11,12</sup> and theoretically<sup>13,14,15,16,17,18,19,20,21</sup>. Apart from the well-known copper oxide superconductors, this family of materials exhibit higher critical temperatures, 26K in  $\text{LaO}_{0.9}\text{F}_{0.1}\text{As}$ <sup>1</sup>, 41K in  $\text{CeO}_{1-x}\text{F}_x\text{FeAs}$ <sup>7</sup>, 43K in  $\text{SmO}_{1-x}\text{F}_x\text{FeAs}$ <sup>10</sup>, and 52K in  $\text{PrO}_{0.89}\text{F}_{0.11}\text{FeAs}$ <sup>11</sup>, as well as 25K in hole doped  $\text{La}_{1-x}\text{Sr}_x\text{OFeAs}$ <sup>6</sup>. Very recently, a number of preliminary analyses have been made to unveil the mystery of superconducting nature, such as the multiband superconductivity, unconventional pairing symmetry, electron-doping and hole-doping effects, strong magnetic instability of the normal state. Experiments from the specific heat measurements<sup>3</sup>, point-contact tunneling spectroscopy<sup>4</sup>, and infrared reflectance spectroscopy<sup>7</sup> provided useful information. For example, according to the point-contact tunneling spectroscopy experiment by Shan *et al.*<sup>4</sup>, a remarkable zero-bias conductance peak was observed at the (110) interface, indicating the possible presence of nodal superconductivity. Ou *et al.*<sup>12</sup> performed angle-integrated photoemission spectroscopy measurements and their data provided certain support for the existence of SDW ordering and an indication of unconventional superconductivity. In the theoretical aspect, the nature of unconventional superconductivity and the pairing mechanism have also been explored preliminarily by several groups based on the density functional theory (DFT) and dynamic mean field theory (DMFT)<sup>15,16,17,18,19</sup>. It was pointed out that the electron-phonon interaction in this system may be too weak to lead such high critical temperatures<sup>20</sup>. Dai *et al.* suggested the appearance of  $p$ -wave triplet superconductivity<sup>21</sup>.

In this paper, we propose a minimal two-band BCS-type Hamiltonian with an effective interband Hubbard interaction term included to model the system. The construction of our model Hamiltonian is based on band structure calculation results and intuitive physical pictures. Taking into account the main features of fermi surface for the undoped material calculated from the DFT and to capture the essential physics of the superconductivity and magnetism in the present system, we adopt a minimal version of the Fermi surface on a primary two-dimensional square lattice in the Fe-Fe plane: one hole band around  $\Gamma$  and one electron band around  $M$  points, both crossing the Fermi surface in the undoped case. Based on rational physical considerations, we introduce an effective interband antiferromagnetic interaction and elucidate that the effective intraband antiferromagnetic coupling could induce the superconducting pairing with a  $d$ -wave symmetry. Our main findings are: (i) the normal state has an SDW order in the undoped case, while upon the charge carrier doping the SDW order drops rapidly and the superconducting order emerges; in particular, analytical results for both SDW and superconducting transition temperatures are explicitly presented, and their respective relations to the SDW and superconducting gaps are elaborated in details, with the former agreeing well with the existing experiment and the latter being quite useful for the future experimental verification; (ii) due to the two-band (electron and hole) superconducting nature of the material, the transition temperature as a function of the effective doping density shows a nearly symmetric electron-hole doping dependence, accounting for the experimental results; (iii) the two-band superconducting state exhibits a  $d$ -wave symmetry. Moreover, we address how to enhance superconducting  $T_c$  in this family of iron-based materials and how to verify our two band model/theory without any fitting parameter.

We start from a minimal two-band model, which captures the essential physics of the multiband unconventional superconducting state and SDW ordering,

$$H = \sum_{k\sigma} \xi_{1k} c_{k\sigma}^\dagger c_{k\sigma} + \sum_{k\sigma} \xi_{2k} d_{k\sigma}^\dagger d_{k\sigma} + U_{eff} \sum_{i,\sigma} n_{1i\sigma} n_{2i\bar{\sigma}} + \sum_{kk'} V_{kk'}^{11} c_{k'\uparrow}^\dagger c_{-k'\downarrow}^\dagger c_{-k\uparrow} c_{k\downarrow} + \sum_{kk'} V_{kk'}^{22} d_{k'\uparrow}^\dagger d_{-k'\downarrow}^\dagger d_{-k\uparrow} d_{k\downarrow} + \sum_{kk'} \left( V_{kk'}^{12} c_{k'\uparrow}^\dagger c_{-k'\downarrow}^\dagger d_{-k\uparrow} d_{k\downarrow} + h.c. \right), \quad (1)$$

where the two band bare dispersions are respectively approximated as  $\xi_{1k} = -\frac{\hbar^2 k^2}{2m_1} + \epsilon_0^{(1)} - \mu$  and  $\xi_{2k} = \frac{\hbar^2 (\mathbf{k}-\mathbf{M})^2}{2m_2} - \epsilon_0^{(2)} - \mu$  ( $\hbar = 1$  hereafter) based on the band calculations<sup>13,14,17,18</sup>, where  $m_1 = 1/t_1$  and  $m_2 = 1/t_2$  are the effective masses of the hole and electron with  $t_{1,2}$  as the effective nearest neighbor hopping integrals in the primary square lattice of sites (with each site as a unit cell consisting of two Fe atoms), which is rotated by the angle of  $\pi/4$  and is enlarged by a factor of  $\sqrt{2} \times \sqrt{2}$  with respect to the reduced Fe-Fe lattice,  $\mu$  is the chemical potential depending on filling, and  $\epsilon_0^{(l)}$  stands for the band offset, where  $l = 1, 2$  represents respectively the nearly filled valence band (hole band) around  $\Gamma = (0, 0)$  and the nearly empty conduction band (electron band) around  $\mathbf{M} = (\pi, \pi)$ , as shown schematically in Fig. 1.  $d_{k\sigma}$  and  $c_{k\sigma}$  are the corresponding electron annihilation operators of bands 1 and 2. For the

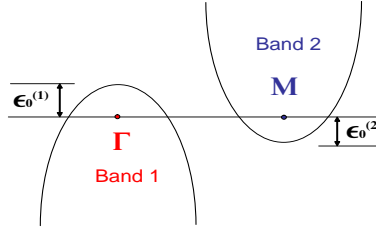


FIG. 1: Schematic plot of the bare band dispersions of the valence (hole) and conduction (electron) band for the undoped parent compound ( $\mu = 0$ ).  $\epsilon_0^{(1,2)}$  determines the initial carrier density before doping.

hole(electron) band, we have the density of states  $\rho_{1,2} = 1/(4\pi t_{1,2})$  with the band width  $W_{h,e} = 1/\rho_{1,2}$ .  $\epsilon_0^{(l)}$  is set to give the carrier density at the undoped case, i.e. the hole density of band-1  $n_h^0 = 2\rho_1 \epsilon_0^{(1)}$ , the electron density of band-2  $n_e^0 = 2\rho_2 \epsilon_0^{(2)}$ , and the effective total electron number per site is  $(2 + n_e^0 - n_h^0)$ .  $V_{kk'}^{11}$  and  $V_{kk'}^{22}$  are the intraband pairing potentials for the two bands.  $V_{kk'}^{12}$  denotes the interband pairing interaction.  $U_{eff}$  represents the effective interband Hubbard interaction term, which will be elaborated in the next paragraph.

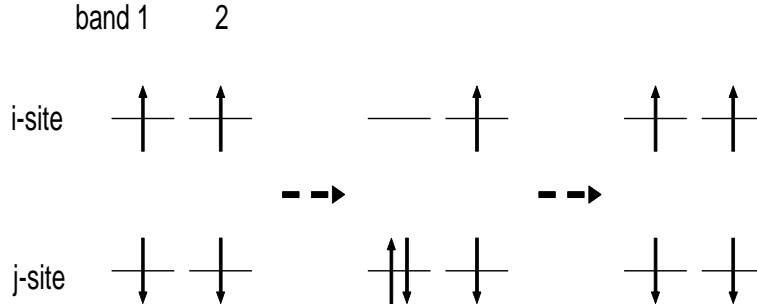


FIG. 2: Schematic representation of the origin of the antiferromagnetic interaction.

It is well known that the superexchange antiferromagnetic coupling derived from the strong coupling of the single-band Hubbard model provides a driving force for the unconventional  $d$ -wave superconducting pairing state in cuprate superconductors. In the present case, the two bands, which involve the Hund's coupling, introduce complications. To understand the main physics, let us simply consider two sites, each having two bands, and four electrons in total. In the absence of hopping, for each site having two electrons, where there are six states, the two lowest energy states have two electrons with the parallel spins in the two different bands (both up or down) due the Hund's coupling of  $J_H$ , while the two relatively higher energy degenerate states have two opposite spins in the two different bands, with the energy difference  $J_H/2$  from the lowest energy level; the rest two states have an even higher energy with opposite spins in either of two bands as the intraband on-site  $U$ -repulsion is stronger than the interband one ( $U'$ ) (Here we refer

to these six states as being in the lower Hubbard band). When the hopping is included, more very high energy states, with each site having at least three electrons, are involved (we refer to these states as being in the upper Hubbard band). If an electron hops from the bare ground state via virtual processes to the upper Hubbard band and then back, which involves an additional intraband  $U$  and corresponds actually to the antiferromagnetic superexchange-like process, lowers the total ground state energy. A typical hopping process is schematically shown in Fig. 1. Analogous to the single-band case, the superexchange-like interaction could also lead to the superconducting pairing interaction with the d-wave pairing symmetry, as in cuprates. For simplicity but with out loss of main physics, here we wish to argue that only the interband term is retained<sup>22</sup> in the effective Hamiltonian (1) after the virtual processes because the intraband  $U$  may be significantly greater than the interband  $U'$ .<sup>23</sup> Since the interband repulsion term lifts the energy  $J_H/2$  above the bare ground state energy level,  $U_{eff}$  is  $\sim J_H/2$ . Below we elaborate first that this  $U_{eff}$ -term can indeed lead to an SDW order at zero or very small electron/hole doping, where the superconducting paring order is suppressed.

The SDW transition temperature  $T_{SDW}$  can be calculated from the following equation<sup>22</sup>

$$1 = U_{eff}\chi_0^{12}(\mathbf{Q}), \quad (2)$$

where  $\chi_0^{12}$  is the interband spin susceptibility

$$\chi_0^{12}(\mathbf{Q}) = \sum_k \frac{f(\xi_{1k}) - f(\xi_{2k+Q})}{\xi_{1k} - \xi_{2k+Q}}, \quad (3)$$

where  $f(\varepsilon)$  is the Fermi-Dirac function  $f(\varepsilon) = 1/(1 + e^{\varepsilon/T_c})$ . To obtain a simple analytic formula of  $T_{SDW}$ , here we set  $m_1 = m_2$  and  $\epsilon_0^{(1)} = \epsilon_0^{(2)} = \epsilon_0$ , where the perfect nesting with vector  $\mathbf{Q} = (\pi, \pi)$  between the two bands occurs at the undoped case ( $\mu = 0$ ), which leads to the SDW instability. Integrating the RHS of Eq. (3), we have an equation for  $T_{SDW}$

$$\frac{T_{SDW}}{W} \approx \frac{2e^\gamma}{\pi} \sqrt{\frac{\epsilon_0}{W} \left(1 - \frac{\epsilon_0}{W}\right)} e^{-\left(\frac{U_{eff}}{W}\right)^{-1}} e^{-1.71\left(\frac{W}{8T_{SDW}}x\right)^2}, \quad (4)$$

where  $\gamma \approx 0.577$  is the Euler constant,  $x$  is the effective small doping, and the condition  $\epsilon_0 \gg T_{SDW}$  has been used. When the electron or hole doping is zero, i.e.  $x = 0$ , we have the largest  $T_{SDW}$ . Remarkably,  $T_{SDW}$  drops drastically whenever more electrons or holes are doped, as seen clearly in Eq.(4) and Fig. 3. If  $m_1 \neq m_2$ ,  $T_{SDW}$  is expected to be lowered.

Below  $T_{SDW}$ , the SDW ordering emerges, whose order parameter may be defined as

$$\Delta_{SDW} = U_{eff} \sum_k \langle c_{k\uparrow} d_{k+Q\downarrow}^\dagger \rangle, \quad (5)$$

where  $\langle \dots \rangle$  denotes thermodynamic average.  $\Delta_{SDW}$  satisfies the following equation

$$1 = U_{eff} \sum_k \frac{f(\eta_{2k} + \Omega_k) - f(\eta_{2k} - \Omega_k)}{2\Omega_k}, \quad (6)$$

where  $\Omega_k = \sqrt{\eta_{1k}^2 + \Delta_{SDW}^2}$ ,  $\eta_{1k} = (\xi_{1k} - \xi_{2k+Q})/2$  and  $\eta_{2k} = (\xi_{1k} + \xi_{2k+Q})/2$ . Here the effective repulsive interaction ( $U_{eff}$ ) between interband electrons may also be viewed as an attractive pairing interaction between electron and hole. Physically, it is noted that the pairing leads to form a "condensate" of bound electron-hole pairs in the triplet state or "excitons"<sup>24</sup>, which exhibits the SDW ordering. The condensate of electron-hole pairs is actually an counterpart of Cooper electron-electron pairs. In this sense, it is straightforward to obtain the famous relation  $2\Delta_{SDW}(0) \approx 3.5T_{SDW}$ , as in the case of the conventional weak-coupling superconductivity. Here we pinpoint out that this relation can be quantitatively verified by independent experimental methods, e.g., the optical conductivity spectra<sup>8</sup> and resistivity or specific heat measurements. As seen from Ref.(8), it may be estimated that  $2\Delta_{SDW}(8K) \approx 350\text{cm}^{-1} = 504K$  and  $T_{SDW} \approx 150K$ , leading to  $2\Delta_{SDW}(8K)/T_{SDW} \approx 3.4$ , which agrees well with the present theory. It is worthwhile noting that, since the effective hopping integrals  $t_{1,2}$  in the present model correspond to those between nearest neighboring sites (unit cells) in the primary lattice, the above SDW ordering pattern is stripe-like antiferromagnetic on the reduced Fe-Fe square lattice, namely, the spin ordering pattern is ferromagnetic in each stripe along the x'(or y')-direction of the reduced Fe-Fe lattice, while it is antiferromagnetic between stripes in the y'(or x')-direction. This kind of SDW ordering was likely observed in a very recent neutron scattering experiment<sup>25</sup>.

At this stage, we turn to address the superconducting ordering. In view of the fact that the SDW order drops very sharply to zero at a very small critical doping, it is reasonable and convenient to ignore the effect of SDW order

on the superconducting ordering above the critical doping level. In the following calculations, the pairing potentials involving two bands are expressed as:  $V_{kk'}^{11} = J_{hh}\gamma_k\gamma_{k'}$ ,  $V_{kk'}^{22} = J_{ee}\gamma_k\gamma_{k'}$  and  $V_{kk'}^{12,21} = J_{he,eh}\gamma_k\gamma_{k'}$ , where  $J_{hh}$ ,  $J_{ee}$ , and  $J_{he,eh}$  are the corresponding coupling constants,  $\gamma_k = \cos k_x - \cos k_y$  in the primary lattice ( $2 \sin k_{x'} \sin k_{y'}$  in the reduced Fe-Fe lattice) is the  $d_{x^2-y^2}$ -wave ( $d_{x'y'}$ -wave) pairing function. Taking the BCS mean field approximation, the quasiparticle eigenspectrum of the  $l$ -th band is then given by  $E_{lk} = \sqrt{\xi_{lk}^2 + |\Delta_l|^2 \gamma_k^2}$ , where  $|\Delta_l|$  is the gap amplitude of the  $l$ -th band ( $l = h, e$ ). They are determined from the following coupled gap equations<sup>26</sup>:

$$\begin{aligned}\Delta_h &= \sum_k \gamma_k (J_{hh} \langle c_{-k\downarrow} c_{k\uparrow} \rangle + J_{he} \langle d_{-k\downarrow} d_{k\uparrow} \rangle), \\ \Delta_e &= \sum_k \gamma_k (J_{ee} \langle d_{-k\downarrow} d_{k\uparrow} \rangle + J_{eh} \langle c_{-k\downarrow} c_{k\uparrow} \rangle).\end{aligned}\quad (7)$$

Then the self-consistent gap equations for  $\Delta_h$  and  $\Delta_e$  read

$$\begin{pmatrix} J_{hh}K_1 & J_{he}K_2 \\ J_{eh}K_1 & J_{ee}K_2 \end{pmatrix} \begin{pmatrix} \Delta_h \\ \Delta_e \end{pmatrix} = \begin{pmatrix} \Delta_h \\ \Delta_e \end{pmatrix}, \quad (8)$$

where  $K_{1,2} = \sum_k \gamma_k^2 \tanh(E_{1,2k}/2T)/E_{1,2k}$  satisfy the following equation

$$\det \begin{pmatrix} J_{hh}K_1 - 1 & J_{he}K_2 \\ J_{eh}K_1 & J_{ee}K_2 - 1 \end{pmatrix} = 0. \quad (9)$$

The superconducting transition temperature  $T_c$  is actually determined from Eq. (9) with  $\Delta_l \rightarrow 0$ , which depends on the pairing interaction strengths and pairing symmetry as well as the normal state dispersions of the two bands.

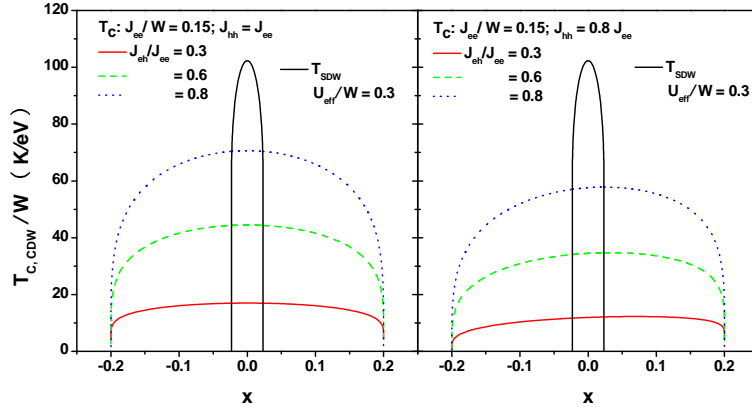


FIG. 3: (Color online) Superconducting critical temperature  $T_c$  and the SDW transition temperature  $T_{SDW}$  as functions of the effective doping  $x$ . The  $T_{SDW}$  curve is calculated from Eq. (4) with the parameters  $U_{eff}/W = 0.3$  and  $\epsilon_0/W = 0.05$ ; the  $T_c$  curves are plotted by simply substituting the relevant reduced parameters into Eq. (10), where  $J_{ee}/W = 0.15$ , and  $|J_{eh}|/J_{ee} = 0.3, 0.6, 0.8$ , respectively for  $J_{hh} = J_{ee}$  and  $J_{hh} = 0.8J_{ee}$ .

Let us first address a more general case:  $J_{ee}, J_{hh} > 0$ , and  $J_{ee}J_{hh} \neq J_{eh}J_{he} > 0$  (noting that  $J_{eh} = J_{he}^*$ ). By the introduction of dimensionless couplings:  $\tilde{J}_{hh,ee} = J_{hh,ee}/W_{h,e}$ ,  $\tilde{J}_{eh,he} = J_{eh,he}/W_{h,e}$ , and  $\tilde{J} = \tilde{J}_{eh}\tilde{J}_{he} - \tilde{J}_{ee}\tilde{J}_{hh}$ , the  $T_c$ -formula is derived as

$$\frac{T_c}{\sqrt{W_e W_h}} = \frac{e^\gamma}{\pi} [n_e n_h (2 - n_e)(2 - n_h)]^{\frac{1}{4}} e^{-\frac{1}{\lambda_{red}}}, \quad (10)$$

with  $\lambda_{red}$  as the reduced pairing strength being given by

$$\lambda_{red}^{-1} = \left\{ \sqrt{\left[ \frac{1}{4} \tilde{J} \ln \frac{n_e(2 - n_e)W_e^2}{n_h(2 - n_h)W_h^2} + \frac{1}{2}(\tilde{J}_{hh} - \tilde{J}_{ee}) \right]^2 + \tilde{J}_{eh}\tilde{J}_{he} - \frac{1}{2}(\tilde{J}_{ee} + \tilde{J}_{hh})} \right\} / \tilde{J}, \quad (11)$$

where  $n_e = n_e^0 + [W_h/(W_e + W_h)]x$  and  $n_h = n_h^0 - [W_e/(W_e + W_h)]x$ , and the condition  $\epsilon_0^{(1,2)} \gg T_c$  has been used. For a special case:  $\widetilde{J}J = 0$ , by taking the limit of  $\widetilde{J}J \rightarrow 0$  in the above equation, the  $T_c$ -formula is reduced to

$$\frac{T_c}{\sqrt{W_e W_h}} = \frac{e^\gamma}{\pi} \left( \sqrt{\frac{W_e}{W_h}} \right)^{\frac{\tilde{J}_{ee} - \tilde{J}_{hh}}{\tilde{J}_{ee} + \tilde{J}_{hh}}} \left[ \sqrt{n_e(2 - n_e)} \right]^{\frac{\tilde{J}_{ee}}{\tilde{J}_{ee} + \tilde{J}_{hh}}} \left[ \sqrt{n_h(2 - n_h)} \right]^{\frac{\tilde{J}_{hh}}{\tilde{J}_{ee} + \tilde{J}_{hh}}} \times e^{-\frac{1}{\tilde{J}_{ee} + \tilde{J}_{hh}}}, \quad (12)$$

In this special case, more intriguingly, it is found from Eq. (8) that the ratio between two gaps  $r(T) = \Delta_h/\Delta_e = J_{he}/J_{ee} = J_{hh}/J_{eh}$ , being independent of temperature and other variables. Therefore, if the ratio value  $|r|$  is experimentally found to be independent of temperature and other variables, it is implied that the system is just in this special case. Note that this result is valid for any two-band superconductivity model described by Eq. (7), regardless of the pairing symmetry.

For a general case, i.e.,  $\widetilde{J}J \neq 0$ , the phase diagram of  $T_c$ - $x$  calculated from above formula is plotted in Fig. 3, where we choose the parameters as  $W_e = W_h = W$  (for simplicity but without loss of generality),  $J_{ee}/W = 0.15$ , and  $\epsilon_0^{(1,2)} = \epsilon_0 = 0.05W$ ,  $U_{eff}/W = 0.3$  (since  $J_H \approx 0.9$  eV, i.e.,  $U_{eff} \sim 0.45$  eV, such choice leads to the effective band width  $W \sim 1.5$  eV, which is not unreasonable in the present system). From Fig. 3, we note that the superconducting order emerges from a very small effective doping and then decays rather slowly to zero at  $x = x_{(e,h)}^c = \pm 2n_{(h,e)}^0$ . When  $J_{ee} = J_{hh}$  and  $n_h^0 = n_e^0$ , the  $T_c$  vs.  $x$  dependence is symmetric for the effective electron and hole doping; while the symmetric feature changes slightly if  $J_{ee}$  (or  $n_h^0$ ) is different from  $J_{hh}$  (or  $n_e^0$ ) not too much (as estimated from the band calculations), in agreement with the experimental result<sup>6</sup>. In particular, if one intraband pairing strength (or the interband coupling) with the largest value is fixed, both the interband coupling (regardless of its sign) and other intraband pairing strength(s) enhance  $T_c$  significantly, reaching the maximum as  $|J_{eh}| \rightarrow J_{hh} \rightarrow J_{ee}$ , whose value is explicitly given by Eq. (12). This feature may be helpful for searching even higher  $T_c$  superconductors in this family of materials, noting that the  $T_c$  record is broken very frequently<sup>1,7,10,11</sup>. Based on our results, another possible way to increase  $T_c$  in this family of superconductors is to increase the effective band width  $W$  (or the effective hopping integral  $t$ ) since we have approximately  $T_c \propto W e^{-\alpha/W}$  with  $\alpha$  being a  $W$ -independent coefficient by noting that  $J_{eh}/W \propto W$ . In this sense, a higher pressure could enhance  $T_c$  as the hopping integral  $t$  is normally increased with the pressure. This expectation was seen in a very recent high pressure experiment that shows clearly the enhancement of  $T_c$  with the shrinkage of the lattice<sup>27</sup>.

The normalized tunneling conductances along the directions (110) and (001) of the primary lattice versus the bias voltage are calculated self-consistently from the gap equations (8) at zero temperature and electron doping at  $x = 0.1$ , as shown in Fig. 4 for a set of parameters used in plotting Fig 3 (except for the upper panel where  $J_{hh} = 0.5J_{ee}$ ). A sharp zero-bias-conductance-peak (ZBCP) along (110) (due the nodal feature of the  $d_{x^2-y^2}$ -wave) and two coherence peaks corresponding to the two gaps (a larger  $\Delta_e^0$  and a smaller  $\Delta_h^0$ ) are clearly seen, as expected. In addition, the two weak kinks in the ZBCP curve can also be seen, which correspond to the two gaps as well. The present ZBCP results are in agreement with the experimental observation reported in Ref.<sup>4</sup>

Finally, we wish to address how to verify unambiguously the present two band model/theory experimentally, without any fitting parameter. From the definitions of  $K_{1,2}$  below Eq. (7), we have  $K_{1,2}(T_c) = \left\{ \ln \sqrt{n_{h,e}(2 - n_{h,e})} - \ln(T_c/W_{h,e}) + C_{T_c} \right\} / W_{h,e}$  and  $K_{1,2}(0) = \left\{ \ln \sqrt{n_{h,e}(2 - n_{h,e})} - \ln(|\Delta_{h,e}^0|/W_{h,e}) + C_0 \right\} / W_{h,e}$ , where  $C_{T_c} = \ln(e^\gamma/\pi) \approx -0.568$  and  $C_0 = (\ln 2 - 1/2) \approx 0.193$  for the present d-wave paring symmetry case. On the other hand, from Eq. (8), we have  $W_{h,e}K_{1,2}(T) = [-\tilde{J}_{ee,hh} + r^{-1,1}(T)\tilde{J}_{he,eh}]/\widetilde{J}J$  for any temperature  $T \leq T_c$ . Combining them, we can find an important relation:

$$\frac{|-\ln(|\Delta_h^0|/T_c) + C_0 - C_{T_c}|}{|-\ln(|\Delta_e^0|/T_c) + C_0 - C_{T_c}|} \times |r_0 r_c| = \frac{W_h}{W_e}, \quad (13)$$

where  $r_{0,c} = r(0), r(T_c)$  are respectively the above introduced gap ratio at zero and transition temperatures. Since the RHS of Eq. (13) depends only on the ratio of the two band widths, this relation can be verified from experimentally measured data for  $|\Delta_{e,h}^0|$  and  $|r_{0,c}|$  at various doping levels and then be used to determine the ratio of  $W_h/W_e$ . Similarly, we can obtain another useful relation:

$$\frac{\ln |r_0|}{[1 + (W_h/W_e)|r_0 r_c|^{-1}](|r_c| - |r_0|)} = \frac{|\tilde{J}_{eh}|}{\widetilde{J}J}. \quad (14)$$

Once  $(W_h/W_e)$  is determined from Eq. (13), this relation can not only be checked by experimental data of  $r_{0,c}$  but also be used to determine the effective interband coupling strength  $|\tilde{J}_{eh}|/\widetilde{J}J$ . It is also interesting to see from

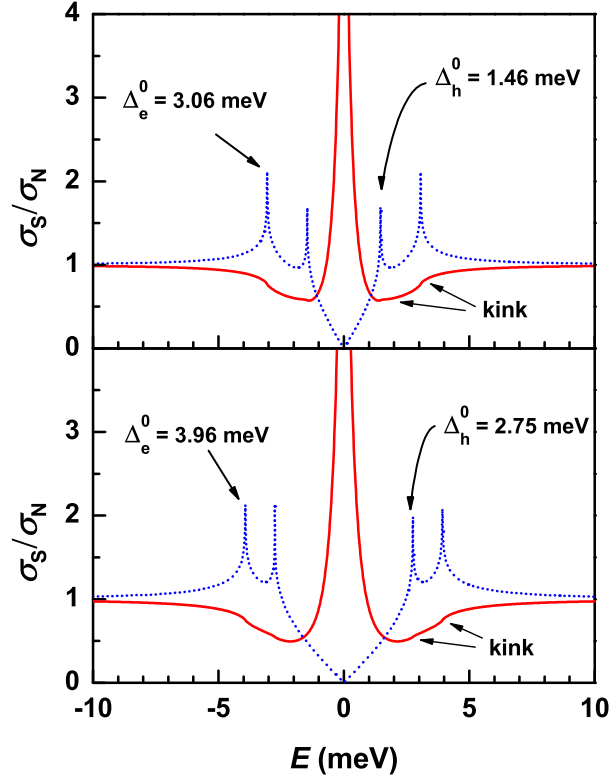


FIG. 4: (Color online) Normalized tunneling conductance as a function of bias voltage at zero temperature for an electron doping at  $x = 0.1$ . The parameters are  $W_h = W_e = 1.5$  eV,  $J_{ee}/W = 0.15$ ,  $|J_{eh}|/J_{ee} = 0.3$  and  $J_{hh}/J_{ee} = 0.8$  for the lower panel, which gives rise to the self-consistent  $\Delta_e^0 = 3.93$  meV and  $\Delta_h^0 = 2.75$  meV; for the upper panel  $J_{hh}/J_{ee} = 0.5$ , which leads to  $\Delta_e^0 = 3.06$  meV and  $\Delta_h^0 = 1.46$  meV.

Eq. (14) that (i) as long as  $|r_0| \approx |r_c|$  is observed experimentally, the system is approximately in the mentioned special case; (ii) if  $|r_0| \approx 1$  is seen experimentally, except the case (i), the interband coupling is negligible, namely, two bands superconduct independently, with the system  $T_c$  being determined by the band having a higher one. It is notable that the above results are also valid for the two-band s-wave superconductors, except for a different constant term  $(C_0 - C_{T_c})_s \approx 0.568$ .

We gratefully acknowledge helpful discussions with Profs. H. H. Wen, Y. P. Wang, N. L. Wang, and D. L. Feng. This work was supported by the NSFC grand under Grants Nos. 10674179 and 10429401, the GRF grant of Hong Kong, the Croucher Senior Research Fellowship, and the Universitas 21 Fellowship at HKU.

---

\* Electronic address: zwang@hkucc.hku.hk

<sup>1</sup> Y. Kamihara, *et al.*, J. Am. Chem. Soc. **130**, 3296(2008).

<sup>2</sup> G.F. Chen *et al.*, arXiv: 0803.0128 [cond-mat.supr-con]; X. Zhu *et al.*, arXiv: 0803.1288 [cond-mat.supr-con].

<sup>3</sup> H. Yang *et al.*, arXiv: 0803.0623 [cond-mat.supr-con]; G. Mu *et al.*, arXiv: 0803.0928 [cond-mat.supr-con].

<sup>4</sup> L. Shan *et al.*, arXiv: 0803.2405v2 [cond-mat.supr-con].

<sup>5</sup> A.S. Sefat *et al.*, arXiv: 0803.2439 [cond-mat.supr-con].

<sup>6</sup> H.H. Wen *et al.*, arXiv: Europhys. Lett. **82**, 17009 (2008); arXiv: 0803.3021 [cond-mat.supr-con].

<sup>7</sup> Z. Li *et al.*, arXiv: 0803.2572 [cond-mat.supr-con].

<sup>8</sup> J. Dong *et al.*, arXiv: 0803.3426 [cond-mat.supr-con].

<sup>9</sup> L. Fang *et al.*, arXiv: 0803.3978 [cond-mat.supr-con].

<sup>10</sup> X.H. Chen *et al.*, arXiv:0803.3603 [cond-mat.supr-con].

<sup>11</sup> Z. Ren *et al.*, arXiv:0803.4283 [cond-mat.supr-con].

<sup>12</sup> H.W. Ou *et al.*, arXiv:0803.4328 [cond-mat.supr-con].

- <sup>13</sup> D.J. Singh and M.H. Du, arXiv:0803.0429 [cond-mat.supr-con].
- <sup>14</sup> G. Xu, W. Ming, Y. Yao, X. Dai, and Z. Fang, arXiv:0803.1282 [cond-mat.supr-con].
- <sup>15</sup> I.I. Mazin, D.J. Singh, M.D. Johannes, and M.H. Du, arXiv:0803.2740 [cond-mat.supr-con].
- <sup>16</sup> K. Kuroki, *et al.*, arXiv:0803.3325 [cond-mat.supr-con].
- <sup>17</sup> C. Cao, P. J. Hirschfeld, and H.-P. Cheng, arXiv:0803.3236 [cond-mat.supr-con].
- <sup>18</sup> F. Ma and Z.Y. Lu, arXiv:0803.3236 [cond-mat.supr-con].
- <sup>19</sup> K. Haule, J. H. Shim, and G. Kotliar, arXiv:0803.1279 [cond-mat.str-el].
- <sup>20</sup> L. Boeri, O.V. Dolgov, and A.A. Golubov, arXiv:0803.2703 [cond-mat.super-con].
- <sup>21</sup> X. Dai, Z. Fang, Y. Zhou and F.C. Zhang, arXiv:0803.3982 [cond-mat.supr-con].
- <sup>22</sup> T. M. Rice, Phys. Rev. B **2**, 3619 (1970).
- <sup>23</sup> If  $(U - U') = \delta U \ll U_{eff}$ , the effective on-site intraband repulsion terms  $[(U_{eff} + \delta U) \sum_{i,l,\sigma} n_{li\sigma} n_{li\bar{\sigma}}]$  may need to be considered, which will be addressed elsewhere later.
- <sup>24</sup> T. M. Rice, *et al.*, J. Appl. Phys. **40**, 1337 (1969).
- <sup>25</sup> C. de la Cruz *et al.*, arXiv:0804.xxxx [cond-mat.supr-con].
- <sup>26</sup> H. Suhl, B. T. Matthias, and L. R. Walker, Phys. Rev. Lett. **12**, 552 (1959).
- <sup>27</sup> W. Lu *et al.*, arXiv:0803.4266 [cond-mat.supr-con].